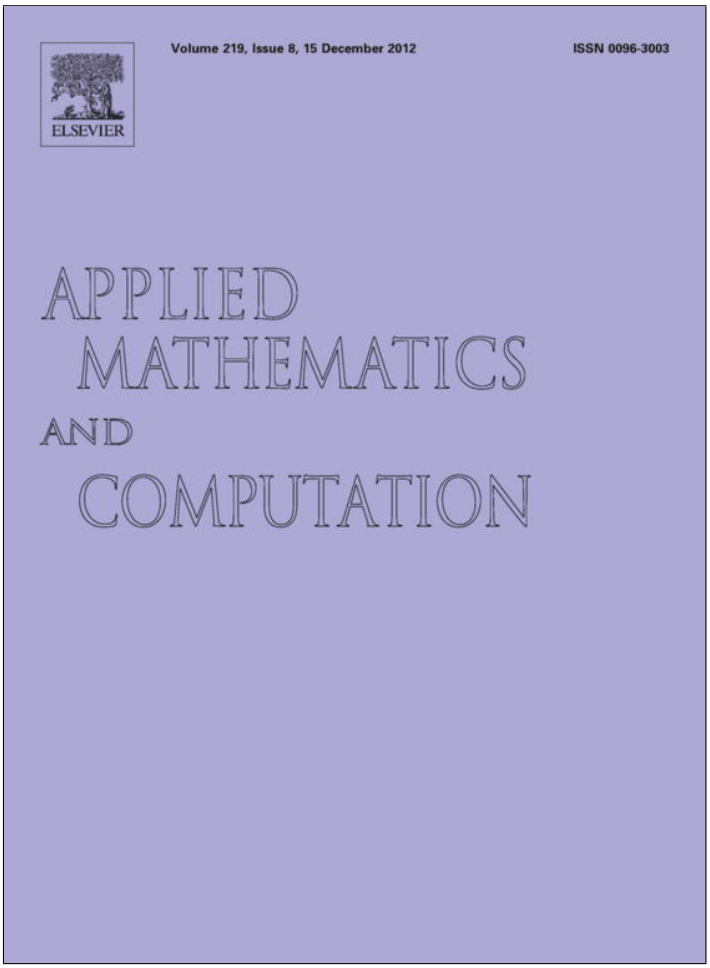

Applied Mathematics and Computation 219 (2012) 3646–3654

Contents lists available at SciVerse ScienceDirect

Applied Mathematics and Computation

journal homepage: www.elsevier.com/locate/amc

Bifurcation diagrams of coupled Schrödinger equations ☆

Michael Essman, Junping Shi *

Department of Mathematics, College of William and Mary, Williamsburg, VA 23187-8795, USA

ARTICLE INFO

Keywords:
Coupled Schrödinger equations
Soliton solution
Ground state
Uniqueness

ABSTRACT

Radially symmetric solutions of many important systems of partial differential equations can be reduced to systems of special ordinary differential equations. A numerical solver for initial value problems for such systems is developed based on Matlab, and numerical bifurcation diagrams are obtained according to the behavior of the solutions. Various bifurcation diagrams of coupled Schrödinger equations from nonlinear physics are obtained, which suggests the uniqueness of the ground state solution.

1. Introduction and background

The nonlinear Schrödinger (NLS) equation

$$i\psi_t + \Delta\psi + \gamma|\psi|^2\psi = 0, \tag{1.1}$$

is a canonical and universal equation which is of major importance in continuum mechanics, plasma physics, nonlinear optics, and condensed matter (where it describes the behavior of a weakly interacting Bose gas and known as the Gross–Pitaevskii (GP) equation). The coupled NLS equations have been receiving a lot of attention with recent experimental advances in multi-component Bose–Einstein condensates (BECs).

Bose–Einstein condensate is a state of matter formed by a system of bosons confined in an external potential and cooled to temperatures very near to absolute zero. Under such supercooled conditions, a large fraction of the atoms collapse into the lowest quantum state of the external potential, at which point quantum effects become apparent on a macroscopic scale. BEC has been an important issue in condensed material physics since the condensate produced by Cornell and Wieman in 1995 [3] using a gas of rubidium atoms cooled to 170 nanokelvin, which was awarded 2001 Nobel Prize in Physics. It is well-known (see [19]) that NLS equations (or GP equations) provide a good description the behavior of the BEC's and is the approach often applied to their theoretical analysis. Phase separation of different types of condenses has been one of recent interests from the experimental work of Cornell and Wieman group in NIST [15,29]. It has also been suggested that multi-component BECs offer the simplest tractable microscopic models in the proper universality class of cosmological systems and solitary waves in multi-component BECs may have their analogs among cosmic strings. The two-component system is described by (see [16,32,33])

$$\begin{cases} i\hbar\frac{\partial\phi_1}{\partial t} = \left(-\frac{\hbar^2}{2m_1}\Delta + V_1(x) + \lambda_1|\phi_1|^2\right)\phi_1 + \beta|\phi_2|^2\phi_1, \\ i\hbar\frac{\partial\phi_2}{\partial t} = \left(-\frac{\hbar^2}{2m_2}\Delta + V_2(x) + \lambda_2|\phi_2|^2\right)\phi_2 + \beta|\phi_1|^2\phi_2, \end{cases} \tag{1.2}$$

☆ This research is supported by NSF CSUMS Grant DMS-0703532 and William and Mary Summer Research Grant.

* Corresponding author.
E-mail addresses: mcessm@wm.edu (M. Essman), shij@math.wm.edu, jxshix@wm.edu (J. Shi).

0096-3003/$ - see front matter © 2012 Elsevier Inc. All rights reserved.
http://dx.doi.org/10.1016/j.amc.2012.09.061

where $x \in \mathbf{R}^n$ for $n = 1, 2, 3$, ϕ_j $(j = 1, 2)$ are the wave functions of two interacting condensates; $V_j(x)$ are the trap potentials; the interaction strengths λ_j and β are determined by the scattering lengths for binary collisions of like and unlike bosons. Another recent interest on coupled NLS is on the propagation of soliton-like pulses in birefringent nonlinear fibers. Experiments have showed the existence of self-trapping of incoherent beam in a nonlinear medium [27,28]. Such findings are significant since optical pulses propagating in a linear medium have a natural tendency to broaden in time (dispersion) and space (diffraction). Such broadening can be eliminated in a nonlinear medium that modifies its refractive index in the presence of light in such a way that dispersion or diffraction effects are counteracted by light-induced lensing. This can allow short pulses to propagate without changing their shape. Mathematically, propagation of solitons in nonlinear fiber couplers is described by the set of coupled nonlinear Schrödinger equations (see [1,14,26]):

$$i\frac{\partial \psi_j}{\partial z} + \frac{1}{2}\frac{\partial^2 \psi_j}{\partial x^2} + \frac{1}{2}\frac{\partial^2 \psi_j}{\partial y^2} + \alpha^2\left(\sum_{j=1}^{K}|\psi_j|^2\right)\psi_j = 0, \tag{1.3}$$

for $j = 1, \ldots, K$. Here (complex-value) ψ_j denotes the jth component of the light beam, α^2 is a coefficient representing the strength of nonlinearity, (x, y) is the transverse coordinate, z is the coordinate along the direction of propagation, and $\sum |\psi_j|^2$ is the change in refractive index profile created by all the incoherent components in the light beam.

In the following we shall only consider (1.2), but (1.3) for $K = 2$ can also be treated similarly. Looking for pulse-like soliton solution of (1.2) in form of

$$\phi_j(t, x) = u_j(x)\exp(i\mu_j t/\hbar), \tag{1.4}$$

we reduce (1.2) to a system of elliptic PDEs:

$$\begin{cases} \frac{\hbar^2}{2m_1}\Delta u_1 + V_1(x)u_1 + \lambda_1|u_1|^2u_1 + \beta|u_2|^2u_1 = \mu_1 u_1, \\ \frac{\hbar^2}{2m_2}\Delta u_2 + V_2(x)u_2 + \lambda_2|u_2|^2u_2 + \beta|u_1|^2u_2 = \mu_2 u_2. \end{cases} \tag{1.5}$$

From a variational consideration, μ_j can be viewed as chemical potential. When $V_j \equiv 0$, the solutions of the homogeneous equation (1.5) are the *canonical ground states*. For the case of $n = 1$, the canonical ground states can be integrated for some parameters.

Driven by the fascinating experiments of BECs and nonlinear optics, the coupled NLS equations have been extensively investigated by theoretical physicists as the main underlying theory in the last decade. Numerical simulations have produced results matching experimental data very well. Variational structure have been observed, but exact soliton solutions are hard to obtain, especially for the higher spatial dimension case. Rigorous mathematical studies about the soliton solutions only start in recent years. Consider the equation of canonical (homogeneous) soliton

$$\begin{cases} \Delta u_1 - \lambda_1 u_1 + \mu_1 u_1^3 + \beta u_1 u_2^2 = 0, & x \in \mathbf{R}^n, \\ \Delta u_2 - \lambda_2 u_2 + \mu_2 u_2^3 + \beta u_1^2 u_2 = 0, & x \in \mathbf{R}^n, \end{cases} \tag{1.6}$$

where $\lambda_i, \mu_i, \beta > 0$, and $n = 1, 2, 3$. We look for positive solutions of (1.6) which decay to zero as $|x| \to \infty$. It is known that such solutions are radially symmetric and decay exponentially [8]. Hence the system to be considered is

$$\begin{cases} \Delta u_1 - \lambda_1 u_1 + \mu_1 u_1^3 + \beta u_1 u_2^2 = 0, & x \in \mathbf{R}^n, \\ \Delta u_2 - \lambda_2 u_2 + \mu_2 u_2^3 + \beta u_1^2 u_2 = 0, & x \in \mathbf{R}^n, \\ u_1(x) > 0,\ u_2(x) > 0, & x \in \mathbf{R}^n, \\ u_1(x) \to 0,\ u_2(x) \to 0, & |x| \to \infty. \end{cases} \tag{1.7}$$

The existence of positive solutions of (1.7) have been considered in several papers recently by Amrosetti and Colorado [2], Bartsch, Dancer, Wang and Wei [4–6,12], Chang and Liu [9], de Figueiredo and Lopez [13], Lin and Wei [20,21], Liu and Wang [22], Maia et al. [23,24], Sirakov [31], Wei and Weth [34–36] and many others. The methods involved in most of these work are variational ones, as the solution (u_1, u_2) of (1.6) are the critical points of the energy function

$$E(u_1, u_2) = \frac{1}{2}\int_{\mathbf{R}^n}(|\nabla u_1|^2 + |\nabla u_2|^2 + \lambda_1 u_1^2 + \lambda_2 u_2^2) - \frac{1}{4}\int_{\mathbf{R}^n}(\mu_1 u_1^4 + 8\beta u_1^2 u_2^2 + \mu_2 u_2^4). \tag{1.8}$$

Bifurcation theory and spectral methods are also used in [4,6,12].

On the other hand, since the solutions of (1.7) are radially symmetric, then they satisfy

$$\begin{cases} u_1'' + \frac{n-1}{r}u_1' - \lambda_1 u_1 + \mu_1 u_1^3 + \beta u_1 u_2^2 = 0, & r > 0, \\ u_2'' + \frac{n-1}{r}u_2' - \lambda_2 u_2 + \mu_2 u_2^3 + \beta u_1^2 u_2 = 0, & r > 0, \\ u_1'(0) = 0,\ u_1'(r) < 0,\ \lim_{r\to\infty} u_1(r) = 0, \\ u_2'(0) = 0,\ u_2'(r) < 0,\ \lim_{r\to\infty} u_2(r) = 0. \end{cases} \tag{1.9}$$

In particular the solution satisfies the initial value problem:

$$\begin{cases} u_1'' + \frac{n-1}{r}u_1' - \lambda_1 u_1 + \mu_1 u_1^3 + \beta u_1 u_2^2 = 0, \quad r > 0, \\ u_2'' + \frac{n-1}{r}u_2' - \lambda_2 u_2 + \mu_2 u_2^3 + \beta u_1^2 u_2 = 0, \quad r > 0, \\ u_1(0) = A > 0, \ u_1'(0) = 0, \\ u_2(0) = B > 0, \ u_2'(0) = 0. \end{cases} \tag{1.10}$$

In this article, we consider the initial value problem (1.10) and its generalization numerically. We give the basic mathematical setting in Section 2; we introduce our numerical method in Section 3; and we present numerical bifurcation diagrams for (1.10) and some observations in Section 4. Our results indicate that for all parameters in (1.9) investigated, the positive solution of (1.9) is *unique*. This has not been proved for general coupled Schrödinger equations, and we hope our numerical investigation can motivate future research in that direction. More discussion on that aspect is provided at the end of Section 4.

2. Mathematical setting

We consider the initial value problem (1.10). The local existence and uniqueness of the solution to (1.10) can be proved via a standard application of contraction mapping principle, see for example, [30] Lemma 2.1. We denote the solution of (1.10) by $(u_1(r;A,B), u_2(r;A,B))$ or simply $(u_1(r), u_2(r))$ when there is no confusion. The solution $(u_1(r), u_2(r))$ can be extended to a maximal interval $(0,R)$ so that $u_1(r) > 0$ and $u_2(r) > 0$ in $(0,R)$. Note that this includes the case that $(u_1(r), u_2(r))$ extended to $r = R$ and $u_1(R)u_2(R) = 0$.

We look for two types of solutions. If

$$u_1(r) > 0, \quad u_2(r) > 0, \quad u_1'(r) < 0, \quad u_2'(r) < 0, \quad 0 < r < \infty, \tag{2.1}$$

then $(u_1(r), u_2(r))$ is a *ground state solution*; if

$$\begin{aligned} &u_1(r) > 0, \quad u_2(r) > 0, \quad u_1'(r) < 0, \quad u_2'(r) < 0, \quad 0 < r < R, \\ &u_1(R) = u_2(R) = 0, \end{aligned} \tag{2.2}$$

then $(u(r), v(r))$ is a *crossing solution*. From the result of [8], any solution of (1.7) is radially symmetric thus a solution of (1.10) satisfying (2.1), and any solution on a ball B_R is also radially symmetric thus a solution of (1.10) satisfying (2.2).

Define

$$\begin{aligned} &f(u_1,u_2) \equiv -\lambda_1 u_1 + \mu_1 u_1^3 + \beta u_1 u_2^2, \\ &g(u_1,u_2) \equiv -\lambda_2 u_2 + \mu_2 u_2^3 + \beta u_1^2 u_2, \\ &\text{and } F(u_1,u_2) = \frac{1}{2}(\lambda_1 u_1^2 + \lambda_2 u_2^2) + \frac{1}{4}(\mu_1 u_1^4 + 8\beta u_1^2 u_2^2 + \mu_2 u_2^4). \end{aligned} \tag{2.3}$$

Then it is easy to verify that $\partial F/\partial u_1 = f$ and $\partial F/\partial u_2 = g$, hence the coupled Schrödinger equations is a gradient system. The set $\{f(u_1,u_2) = 0\}$ consists of the line $\{u_1 = 0\}$ and the ellipse $E_1 = \{\mu_1 u_1^2 + \beta u_2^2 = \lambda_1\}$, and the set $\{g(u_1,u_2) = 0\}$ consists of the line $\{u_2 = 0\}$ and the ellipse $E_2 = \{\beta u_1^2 + \mu_2 u_2^2 = \lambda_2\}$. Let

$$\beta_1 = \min\left\{\frac{\lambda_2}{\lambda_1}\mu_1, \frac{\lambda_1}{\lambda_2}\mu_2\right\}, \quad \text{and} \quad \beta_2 = \max\left\{\frac{\lambda_2}{\lambda_1}\mu_1, \frac{\lambda_1}{\lambda_2}\mu_2\right\}. \tag{2.4}$$

Then it is easy to show that when $0 < \beta < \beta_1$ and $\beta > \beta_2$, E_1 and E_2 intersects exactly once in the first quadrant; and when $\beta_1 < \beta < \beta_2$, E_1 and E_2 do not intersect hence one ellipse is inside the other one (see Fig. 1). In the first case, the unique intersection point of $f = 0$ and $g = 0$ is the global minimum of the potential function $F(u_1,u_2)$ in the first quadrant. We assume

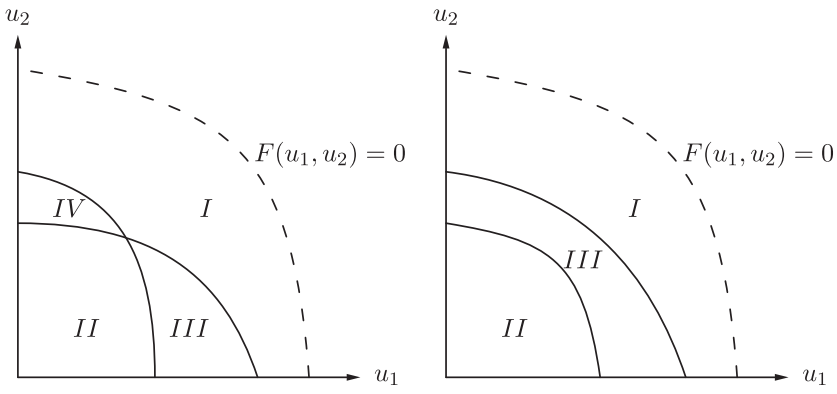

Fig. 1. The regions of possible initial values (A,B): solid lines are $f(u_1,u_2) = 0$ and $g(u_1,u_2) = 0$ respectively; and the dashed line is $F(u_1,u_2) = 0$. (left): $0 < \beta < \beta_1$ and $\beta > \beta_2$; (right) $\beta_1 < \beta < \beta_2$.

that $\min F(u_1,u_2) = -\gamma_1 < 0$. Define $F_\gamma = \{(u_1,u_2) \in \mathbf{R}^2_+ : F(u_1,u_2) \leqslant \gamma\}$, then there exists $0 < \gamma_2 < \gamma_1$ such that when $-\gamma_1 < \gamma < -\gamma_2, F_\gamma$ is a connected closed subset.

According to the signs of f and g, we define the following regions in $\mathbf{R}^2_+$:

$$\begin{aligned} I &= \{(u_1,u_2) \in \mathbf{R}^2_+ : f(u_1,u_2) > 0, g(u_1,u_2) > 0\},\\ II &= \{(u_1,u_2) \in \mathbf{R}^2_+ : f(u_1,u_2) < 0, g(u_1,u_2) < 0\},\\ III &= \{(u_1,u_2) \in \mathbf{R}^2_+ : f(u_1,u_2) < 0, g(u_1,u_2) > 0\},\\ IV &= \{(u_1,u_2) \in \mathbf{R}^2_+ : f(u_1,u_2) > 0, g(u_1,u_2) < 0\}. \end{aligned} \tag{2.5}$$

For $(A,B) \in II \cup III \cup IV$, $u' > 0$ or $v' > 0$ in $(0,\delta)$ for small $\delta > 0$, hence it cannot be a ground state or a crossing solution. For $(A,B) \in I$, $u' < 0$ and $v' < 0$ in $(0,\delta)$ for small $\delta > 0$, thus

$$T = T(A,B) = \sup\{t > 0 : u_1(r) > 0, u_2(r) > 0, u_1'(r) < 0, u_2'(r) < 0, r \in (0,t)\}$$

exists. We partition I into the following classes:

$$\begin{aligned} \mathcal{B} &= \{(A,B) \in I : T < \infty, u_1(T) = 0, u_1'(T) < 0, u_2(T) > 0, u_2'(T) < 0\},\\ \mathcal{G} &= \{(A,B) \in I : T < \infty, u_1(T) > 0, u_1'(T) = 0, u_2(T) > 0, u_2'(T) < 0\},\\ \mathcal{R} &= \{(A,B) \in I : T < \infty, u_1(T) > 0, u_1'(T) < 0, u_2(T) = 0, u_2'(T) < 0\},\\ \mathcal{Y} &= \{(A,B) \in I : T < \infty, u_1(T) > 0, u_1'(T) < 0, u_2(T) > 0, u_2'(T) = 0\},\\ \mathcal{S} &= \{(A,B) \in I : T < \infty, u_1(T) = 0, u_1'(T) < 0, u_2(T) = 0, u_2'(T) < 0\},\\ \mathcal{Q} &= \{(A,B) \in I : T = \infty, \lim_{r\to\infty} u_1(r) = \lim_{r\to\infty} u_2(r) = 0\},\\ \mathcal{P} &= I \setminus (\mathcal{B} \cup \mathcal{G} \cup \mathcal{R} \cup \mathcal{Y} \cup \mathcal{S} \cup \mathcal{Q}). \end{aligned} \tag{2.6}$$

One can show that each of $\mathcal{B},\mathcal{G},\mathcal{R},\mathcal{Y}$ is an open subset of $\mathbf{R}^2_+$ if it is non-empty. Indeed if $(A_0,B_0) \in \mathcal{B}$, then the solution starting from (A_0,B_0) can be extended to $T+\epsilon$ so that $u_1(T+\epsilon) < -\delta, u_1'(T+\epsilon) < -\delta, u_2(T+\epsilon) > \delta$ and $u_2'(T+\epsilon) < -\delta$ for some $\delta > 0$. Then there exists a neighborhood O of (A_0,B_0), such that for any (A,B) in O, we have $u_1(T+\epsilon) < -\delta/2$, $u_1'(T+\epsilon) < -\delta/2, u_2(T+\epsilon) > \delta/2$ and $u_2'(T+\epsilon) < -\delta/2$. Then apparently such (A,B) also belongs to $\mathcal{B}$. The proof for the openness of $\mathcal{G},\mathcal{R},\mathcal{Y}$ is similar. The set $\mathcal{S}$ is the boundary between $\mathcal{B}$ and $\mathcal{R}$ representing the initial values for crossing solutions, and the crossing time T satisfies $u_1(T) = u_2(T) = 0$; and each element in $\mathcal{Q}$ represents a ground state solution. The set $\mathcal{S} \cup \mathcal{Q} \cup \mathcal{P}$ is closed in $\mathbf{R}^2_+$ as it is the complement of $\mathcal{B} \cup \mathcal{G} \cup \mathcal{R} \cup \mathcal{Y}$. Solution curves of type $\mathcal{B},\mathcal{S}$ and $\mathcal{R}$ are illustrated in Fig. 2.

3. Numerical methods

We use a computational method to solve an initial value problem like (1.10). Indeed we consider a more general problem:

$$\begin{cases} u_1'' + \frac{n-1}{r}u_1' + f(u_1,u_2) = 0, & r > 0,\\ u_2'' + \frac{n-1}{r}u_2' + g(u_1,u_2) = 0, & r > 0,\\ u_1(0) = A > 0,\ u_1'(0) = 0,\\ u_2(0) = B > 0,\ u_2'(0) = 0, \end{cases} \tag{3.1}$$

where f,g are appropriate nonlinear functions, and $A,B > 0$. We first expand the system (3.1) from two second order differential equations into a system of four first order differential equations

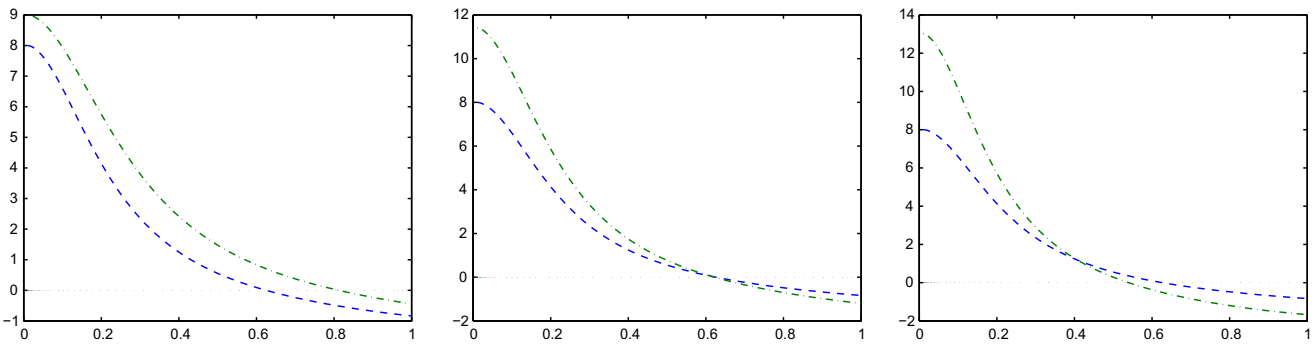

Fig. 2. Solution curves of (1.10) when $n = 3$, $\mu_1 = \lambda_1 = \lambda_2 = 1$, $\mu_2 = 2$, $\beta = 0.01$. Initial values: $u(0) = 8$ in all three; (left) $v(0) = 9$ ($u(R) = 0$ and $v(R) > 0$); (middle) $v(0) = 11.4$ ($u(R) = v(R) = 0$, crossing solution); (right) $v(0) = 13$ ($u(R) > 0$ and $v(R) = 0$).

$$\begin{cases} u_1' = v_1, \\ v_1' = -\frac{n-1}{r}u_1' - f(u_1,u_2), \\ u_2' = v_2, \\ v_2' = -\frac{n-1}{r}u_2' - g(u_1,u_2), \\ u_1(0) = A > 0, \;\; v_1(0) = 0, \\ u_2(0) = B > 0, \;\; v_2(0) = 0. \end{cases} \tag{3.2}$$

We discretize the space of initial values $\{(A,B) : A_b \leqslant A \leqslant A_e, B_b \leqslant B \leqslant B_e\}$ to a two-dimensional data structure:

$$\{(A_i,B_j) : 0 \leqslant i \leqslant n, \;\; 0 \leqslant j \leqslant m\},$$

where $A_i = A_b + (i/n)(A_e - A_b)$ and $B_j = B_b + (j/n)(B_e - B_b)$. Then for each initial value (A_i,B_j), we solve (3.2) by using an appropriate ODE solver in `Matlab`, until the solution reaches a stopping time which is defined as

$$T = \sup\{r > 0 : u_1(r)v_1(r)u_2(r)v_2(r) \neq 0\}. \tag{3.3}$$

In fact, we only detect the stopping time if the initial value (A,B) is valid, which means that it satisfies

$$f(A,B) > 0 \quad \text{and} \quad g(A,B) > 0. \tag{3.4}$$

That is, if (A,B) belongs to region I defined in (2.5). If $(A,B) \in II \bigcup III \bigcup IV$, then initially $u'(r) > 0$ or $v'(r) > 0$ for small $r > 0$, and the solution cannot be the one we desire. On the bifurcation graph, we use color "cyan" for the data point (A_i,B_j) if $(A_i,B_j) \in II \bigcup III \bigcup IV$.

On the other hand, if the initial value $(A_i,B_j) \in I$, then for some $\delta > 0, u_1(r), u_2(r) > 0$ and $u_1'(r), u_2'(r) < 0$ for $r \in (0,\delta)$, hence T is well-defined. As the solution reaches T, we color the data point according to the classification in (2.6): "blue" for $u_1(T) = 0$; "green" for $u_1'(T) = 0$; "red" for $u_2(T) = 0$; and "yellow" for $u_2'(T) = 0$. Notice that it is certainly possible to have two values equaling zero simultaneously, but in general such initial values (A,B) only form boundary curves on $\mathbf{R}^2_+$ between the open subsets $\mathcal{B},\mathcal{G},\mathcal{R},\mathcal{Y}$ and the cyan region $\mathcal{C} = II \bigcup III \bigcup IV$.

On a bifurcation diagram (see for example, Fig. 3), the cyan[1] area is bordered by the highlighted curves of $f(u,v) = 0$ and $g(u,v) = 0$. We also point out that, the boundary curve between the red and blue regions gives all initial values for *crossing solution* for which $u_1(T) = u_2(T) = 0$; the boundary curve between the yellow and green regions gives all initial values for which $u_1'(T) = u_2'(T) = 0$, which indeed gives all radially symmetric solutions satisfying Neumann boundary condition on a sphere with $|x| = T$. In all diagrams in Fig. 3, there is at most one common point for all four (red, blue, green, yellow) regions, and that point is exactly the one corresponding to the *ground state solution*. Note that (3.1) cannot have solution with $u_1(T) = u_2(T) = u_1'(T) = u_2'(T) = 0$ for finite T from the uniqueness of solution to ODE.

4. Numerical bifurcation diagrams

By using the numerical scheme described in Section 3, we investigate the distribution of the qualitative behavior of solutions to the shooting problem (3.1). For the numerical calculation, we use the `Matlab` solver *ode113* since it handles computationally intensive problems well with an acceptable degree of accuracy. The calculation of the initial value problem is preformed for initial value (A,B) in a rectangle $[0,A_{max}] \times [0,B_{max}]$. In Figs. 3 and 4(a), we choose $A_{max} = B_{max} = 10$, and in other diagrams of Fig. 4, we choose $A_{max} = B_{max} = 5$. In each diagram, we sample 300^2 points to color according to the algorithm above, hence each bifurcation diagram is a five-color dot matrix with 9×10^4 dots.

From the discussion of the nonlinearities $f(u,v)$ and $g(u,v)$ in coupled Schrödinger equations in Section 2, one can identify two possible bifurcation points

$$\beta_1 = \min\left\{\frac{\lambda_2}{\lambda_1}\mu_1, \frac{\lambda_1}{\lambda_2}\mu_2\right\}, \quad \text{and} \quad \beta_2 = \max\left\{\frac{\lambda_2}{\lambda_1}\mu_1, \frac{\lambda_1}{\lambda_2}\mu_2\right\}.$$

In [2,6,13], two other possible bifurcation points are identified. Let ϕ_a be the unique positive radially symmetric solution of

$$\begin{cases} \Delta\phi - a\phi + \phi^3 = 0, & x \in \mathbf{R}^n, \\ \phi(x) \to 0, & |x| \to \infty, \end{cases} \tag{4.1}$$

and for $\eta > 0$ define

$$-v_1(\eta) = \text{principal eigenvalue of the operator } M_0(k) = -\Delta k - \eta\phi_0^2 k. \tag{4.2}$$

For the existence and uniqueness of ϕ_a, we refer to [7]. It is also known [7] that M_0 has a unique positive eigenvalue $v_1(\eta)$, and the property of $v_1(\eta)$ can be found in [13]. Then Theorem 1.1 of [13] (see also [6]) shows that when $n = 1,2,3$, there exist $0 < \beta_1^* < \beta_2^* < \infty$ such that when $0 < \beta < \beta_1^*$ and $\beta > \beta_2^*$, (1.7) has a solution. Here if $\lambda_1 = 1$, then β_i^* satisfy

[1] For interpretation of color in Fig. 3, the reader is referred to the web version of this article.

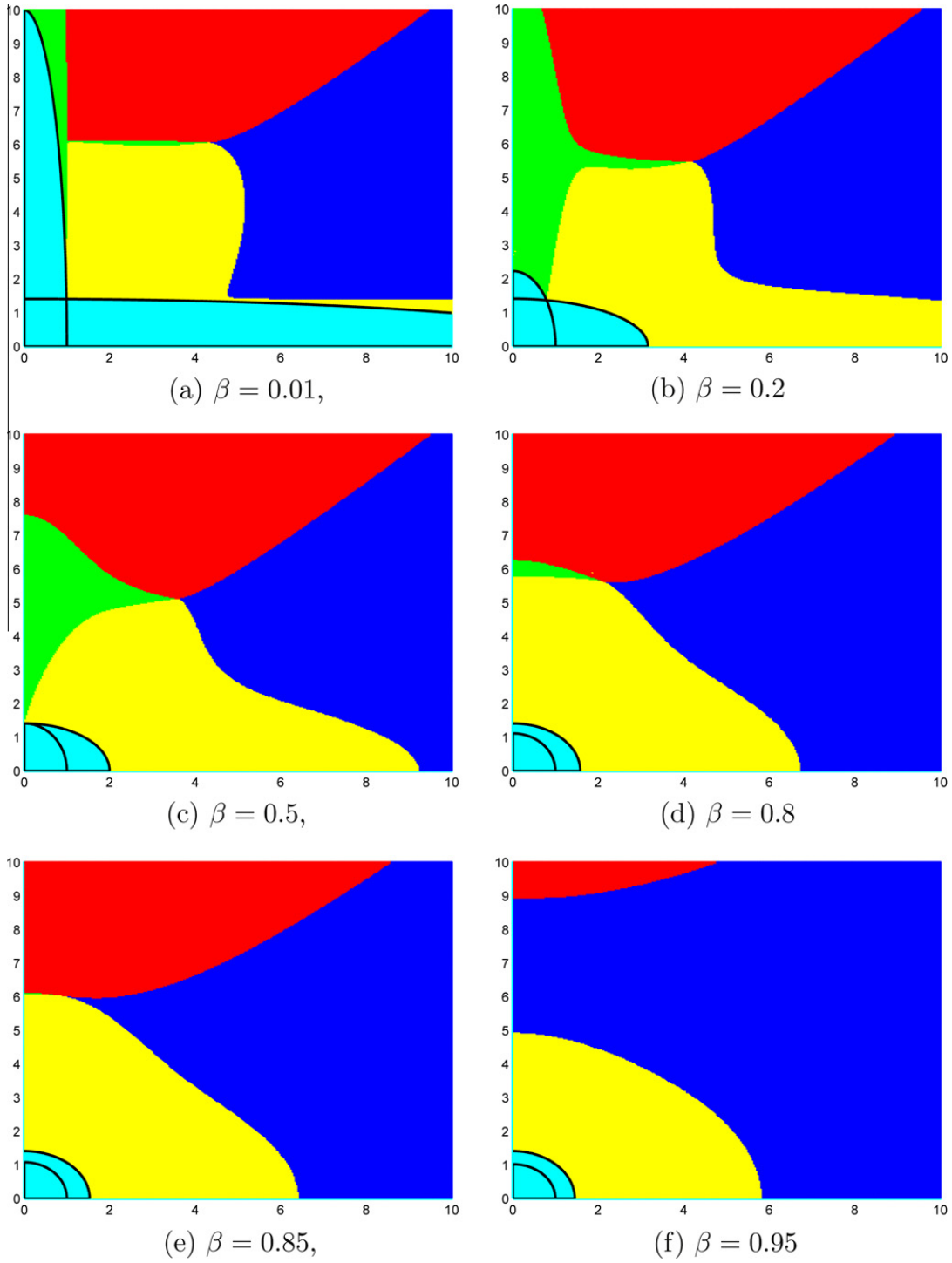

Fig. 3. Bifurcation diagrams of (1.10). The coordinates are (A, B), the initial values in (3.1). Here $0 \leqslant A, B \leqslant 10$, 300×300 points in $(A, B) \in [0, 10]^2$ are sampled, $n = 3,\ \mu_1 = \mu_2 = 1,\ \lambda_1 = 1,\ \lambda_2 = 2$.

$$\begin{aligned} &\beta_1^* = \min\{\beta_a, \beta_b\}, \quad \beta_1^* = \max\{\beta_a, \beta_b\}, \\ &\text{where } v_1(\frac{\beta_a}{\mu_1}) = \lambda_2, \quad v_1(\frac{\beta_b}{\mu_2}) = \frac{1}{\lambda_2}. \end{aligned} \tag{4.3}$$

One can show that (see [13] Theorems 1.2 and 1.3)

$$0 < \beta_1 < \beta_1^* < \beta_2^* < \beta_2.$$

This existence result can be shown from our numerical bifurcation diagrams of the shooting problem (3.1). In our numerical experiment, we fix a set of parameters $(\lambda_1, \lambda_2, \mu_1, \mu_2) = (1, 2, 1, 1)$ and $n = 3$, and use β as a free parameter. Hence $\beta_1 = 0.5$ and $\beta_2 = 2$. In Fig. 3, one can see that $\beta_1^* \approx 0.85$. As $\beta \to (\beta_1^*)^-$, the green region (for which $u_1'(T) = 0$) shrinks to

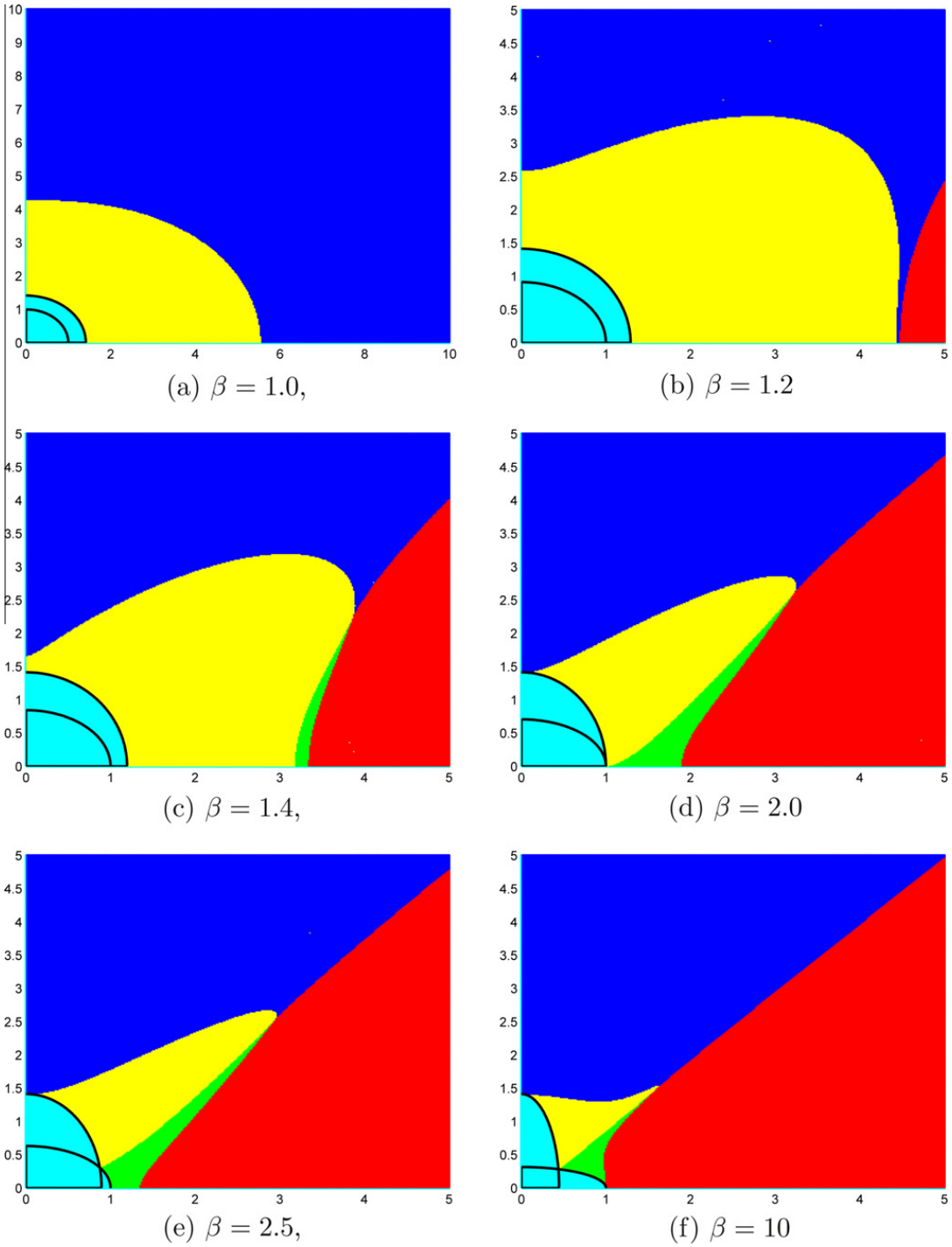

Fig. 4. Bifurcation diagrams of (1.10). The coordinates are (A, B), the initial values in (3.1). Here (except (a)) $0 \leqslant A, B \leqslant 5$, 300×300 points in $(A, B) \in [0, 5]^2$ are sampled, $n = 3$, $\mu_1 = \mu_2 = 1$, $\lambda_1 = 1$, $\lambda_2 = 2$. In (a), $0 \leqslant A, B \leqslant 10$.

empty near $(A, B) = (0, 6)$. This indicates a convergence of the ground states of the system to the semitrivial state $(u_1(r), u_2(r)) = (0, \phi_2)$, where ϕ_2 is the unique solution of (4.1) with same λ_2. From Fig. 5, $\phi_2(0) \approx 6.13$. This also confirms the bifurcation diagram suggested in [2,6].

In Fig. 3, one can see that the structure of the bifurcation diagrams undergoes several topological change as β increases from $\beta = 0$ to $\beta = 1$. When $0 < \beta < \beta_1$, the cyan region borders the green region by the curve $-1 + u_1^2 + \beta u_2^2 = 0$, and borders the yellow region by the curve $-2 + u_2^2 + \beta u_1^2 = 0$. Hence the boundary curve between red–green region and blue–yellow region connects with the unique intersection point of $-1 + u_1^2 + \beta u_2^2 = 0$ and $-2 + u_2^2 + \beta u_1^2 = 0$ (see Fig. 3(a) and (b)). For $\beta_1 < \beta < \beta_1^*$, only the yellow region encircles the non-admissible region (cyan) in the lower-left corner, and the yellow region also shares a boundary with u_2-axis while the green region shrinks (see Fig. 3(c) and (d)). For $\beta > \beta_1^*$, the blue region reaches the vertical boundary u_2-axis, and it separates the yellow and red regions (see Fig. 3(e) and (f)).

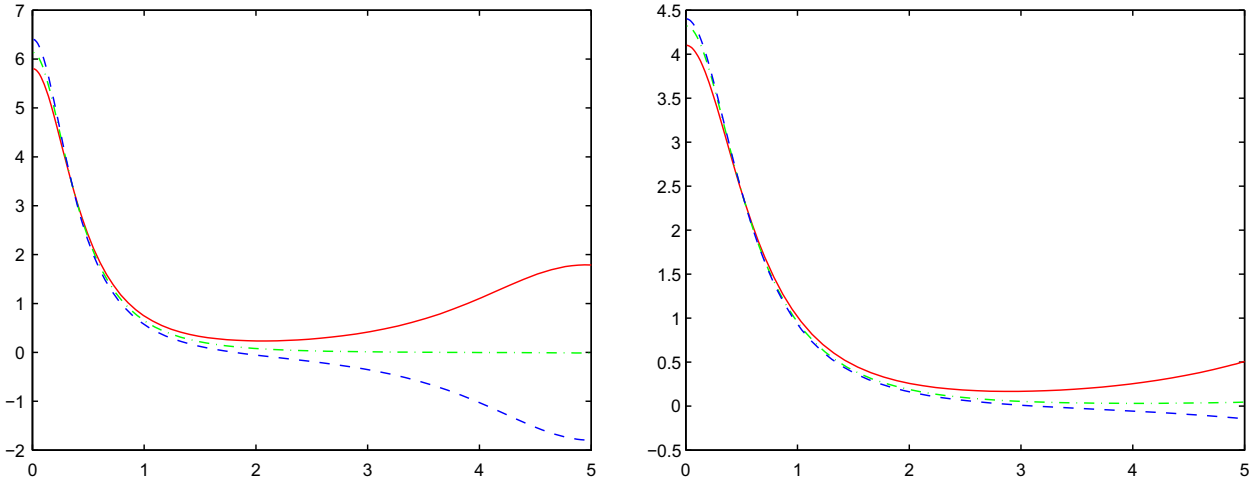

Fig. 5. Ground state of (4.1) when $n = 3$. (left) $a = 2$, ground state $\phi_2(0) \approx 6.13$; (right) $a = 1$, ground state $\phi_1(0) \approx 4.32$.

For $\beta_1^*(\approx 0.85) < \beta_1 < \beta_2^*(\approx 1.2)$, it has been conjectured that (1.7) has no ground state solution. Fig. 3(f) appears to support that claim as the green region (where $u_1'(T) = 0$) is empty for this parameter range. At $\beta = 1$, the red region is also absent on the diagram (even if we enlarge the plotting region). Hence the bifurcation diagram completely consists of blue[2] and yellow regions when $\beta = 1$ (see Fig. 4(a)).

As β increases from $\beta = 1$, a similar sequence of bifurcations occurs, see Fig. 4(b)–(f). Here we use the plotting window $(A, B) \in [0, 5] \times [0, 5]$ for a better viewing area. The red region reappears as β increases from $\beta = 1$ but from the right lower corner. At $\beta = \beta_2^* \approx 1.2$, the blue region touches off from u_1-axis, which represents the bifurcation from semitrivial solution $(u_1(r), u_2(r)) = (\phi_1, 0)$. From Fig. 5, $\phi_1(0) \approx 4.32$, that is exactly the last touching point of the blue region with u_1-axis (Fig. 4(b)). As β crosses β_2^*, a green region emerges from the u_1-axis, and a ground state bifurcates from the semitrivial solution. Again the ground state is indicated by the unique common point of the four regions (Fig. 4(c)). At $\beta = \beta_2 = 2$ (Fig. 4(d)), the green region reaches to the cyan region of non-admissible initial values, and for $\beta > \beta_2$, the yellow and green regions encircle the non-admissible region in the lower-left corner (Fig. 4(e)). But one can see that when β is large, the yellow and green regions do not share boundary with u_1 and u_2 axes, which is different from the small β case ($\beta = 0.01$ and $\beta = 0.2$ in Fig. 3(a) and (b)).

We also remark that our selection $(\lambda_1, \lambda_2, \mu_1, \mu_2) = (1, 2, 1, 1)$ shows enough of asymmetry for the system displaying various bifurcation diagrams. When $\lambda_1 = \lambda_2$ and $\mu_1 = \mu_2$, the bifurcation diagram is always symmetric: the yellow and green regions are symmetric with respect to $A = B$, and so are the blue and red regions.

Another very degenerate case is when $\beta = \mu_1 = \mu_2 = \lambda_1 = \lambda_2 = 1$, and if z is the unique positive radial solution of $-\Delta z + z = z^3$ in the whole space, then the pair $(\cos(\theta)z(x), \sin(\theta)z(x))$ is a positive solution of the system, for any $\theta \in [0, \pi/2]$, having the same energy (but different initial value), this suggest that, at least in this case, the parameters equality turn the problem into a very degenerate one, which does not possess a unique positive solution (see [17]).

We summarize our observation of numerical bifurcation diagrams and give a few conjectures to possible rigorous approach:

1. The shooting problem (3.1) in general possesses four types of solutions with stopping condition $u_i(T) = 0$ or $u_i'(T) = 0$ for $i = 1, 2$, and the region of each type is an open subset of $\mathbf{R}_+^2$. These four regions cover most of initial values, but the boundary between the regions include ground state and crossing solutions.
2. The absence of at leat one type of regions implies the non-existence of a ground state solution of the coupled Schrödinger equations (1.7), which occurs when $\beta \in (\beta_1^*, \beta_2^*)$. We remark that such a non-existence result has not been proved rigorously for any non-trivial case from our knowledge.
3. The common boundary point of all four regions is a ground state solution of (1.7), and from numerical experiments here, the ground state solution is *unique* for these parameter values. In general, the uniqueness of the ground state of (1.7) is not known except some special case (see [10,17,18,25]), and the nondegeneracy of the ground state is studied in [12]. However the uniqueness may not hold for some parameter values in the degenerate cases.
4. When the ground state exists, a monotone increasing curve in $\mathbf{R}_+^2$ separates the blue–yellow and green–red regions. This curve contains all solutions so that $u_1(T) = u_2(T) = 0$ or $u_1'(T) = u_2'(T) = 0$. The monotonicity of such curve has been proved in some similar problems [10,11], but still remains open for the coupled Schrödinger equations (1.7).

[2] For interpretation of color in Fig. 4, the reader is referred to the web version of this article.

Acknowledgement

We thank an anonymous referee for some helpful comments, including a remark about possible non-uniqueness scenario.

References

[1] Nail Akhmediev, Adrian Ankiewicz, Partially coherent solitons on a finite background, Phys. Rev. Lett. 82 (1999) 2661–2664.
[2] Antonio Ambrosetti, Eduardo Colorado, Standing waves of some coupled nonlinear Schrödinger equations, J. Lond. Math. Soc. (2) 75 (1) (2007) 67–82.
[3] M.H. Anderson, J.R. Ensher, M.R. Matthews, C.E. Wieman, E.A. Cornell, Observation of Bose–Einstein condensation in a dilute atomic vapor, Science 269 (1995) 198–201.
[4] Thomas Bartsch, Norman Dancer, Zhi-Qiang Wang, A Liouville theorem, a-priori bounds, and bifurcating branches of positive solutions for a nonlinear elliptic system, Calc. Var. Partial Differential Equations 37 (3–4) (2010) 345–361.
[5] Thomas Bartsch, Zhi-Qiang Wang, Note on ground states of nonlinear Schrödinger systems, J. Partial Differential Equations 19 (3) (2006) 200–207.
[6] Thomas Bartsch, Zhi-Qiang Wang, Juncheng Wei, Bound states for a coupled Schrödinger system, J. Fixed Point Theory Appl. 2 (2) (2007) 353–367.
[7] Peter W. Bates, Junping Shi, Existence and instability of spike layer solutions to singular perturbation problems, J. Funct. Anal. 196 (2) (2002) 429–482.
[8] Jérôme Busca, Boyan Sirakov, Symmetry results for semilinear elliptic systems in the whole space, J. Differential Equations 163 (1) (2000) 41–56.
[9] Jinyong Chang, Zhaoli Liu, Ground states of nonlinear Schrödinger systems, Proc. Amer. Math. Soc. 138 (2) (2010) 687–693.
[10] Jann-Long Chern, Chang-Shou Lin, Shi Junping, Uniqueness of solution to a coupled cooperative system, preprint.
[11] Jann-Long Chern, Yong-Li Tang, Chang-Shou Lin, Junping Shi, Existence, uniqueness and stability of positive solutions to sublinear elliptic systems, Proc. Roy. Soc. Edinburgh Sect. A 141 (1) (2011) 45–64.
[12] E.N. Dancer, Juncheng Wei, Spike solutions in coupled nonlinear Schrödinger equations with attractive interaction, Trans. Amer. Math. Soc. 361 (3) (2009) 1189–1208.
[13] Djairo G. de Figueiredo, Orlando Lopez, Solitary waves for some nonlinear Schrödinger systems, Ann. Inst. H. Poincaré Anal. Non Linéaire 25 (1) (2008) 149–161.
[14] Akira Hasegawaa, An historical review of application of optical solitons for high speed communications, Chaos 10 (3) (2000) 475–485.
[15] D.S. Hall, M.R. Matthews, J.R. Ensher, C.E. Wieman, E.A. Cornell, Dynamics of component separation in a binary mixture of Bose–Einstein condensates, Phys. Rev. Lett. 81 (1998) 1539–1542.
[16] Tin-Lun Ho, V.B. Shenoy, Binary mixtures of Bose condensates of Alkali atoms, Phys. Rev. Lett. 77 (1996) 3276–3279.
[17] Norihisa Ikoma, Uniqueness of positive solutions for a nonlinear elliptic system, NoDEA Nonlinear Differential Equations Appl. 16 (5) (2009) 555–567.
[18] Congming Li, Li Ma, Uniqueness of positive bound states to Schrödinger systems with critical exponents, SIAM J. Math. Anal. 40 (3) (2008) 1049–1057.
[19] H. Lieb Elliott, Robert Seiringer, Derivation of the Gross–Pitaevskii equation for rotating Bose gases, Comm. Math. Phys. 264 (2) (2006) 505–537.
[20] Tai-Chia Lin, Juncheng Wei, Ground state of N coupled nonlinear Schrödinger equations in Rn, $n \leqslant 3$, Comm. Math. Phys. 255 (3) (2005) 629–653.
[21] Tai-Chia Lin, Juncheng Wei, Spikes in two coupled nonlinear Schrödinger equations, Ann. Inst. H. Poincaré Anal. Non Linéaire 22 (4) (2005) 403–439.
[22] Zhaoli Liu, Zhi-Qiang Wang, Multiple bound states of nonlinear Schrödinger systems, Comm. Math. Phys. 282 (3) (2008) 721–731.
[23] L.A. Maia, E. Montefusco, B. Pellacci, Positive solutions for a weakly coupled nonlinear Schrödinger system, J. Differential Equations 229 (2) (2006) 743–767.
[24] L.A. Maia, E. Montefusco, B. Pellacci, Infinitely many nodal solutions for a weakly coupled nonlinear Schrödinger system, Commun. Contemp. Math. 10 (5) (2008) 651–669.
[25] L. Ma, L. Zhao, Uniqueness of ground states of some coupled nonlinear Schrödinger systems and their application, J. Differential Equations 245 (9) (2008) 2551–2565.
[26] C.R. Menyuk, Pulse propagation in an elliptically birefringent Kerr medium, IEEE J. Quantum Electron. QE-25 (1989) 2674.
[27] M. Mitchell, Z. Chen, M. Shih, M. Segev, Self-trapping of partially spatially incoherent light, Phys. Rev. Lett. 77 (1996) 490–493.
[28] M. Mitchell, M. Segev, Self-trapping of incoherent white light, Nature 387 (1997) 880–883.
[29] C.J. Myatt, E.A. Burt, R.W. Ghrist, E.A. Cornell, C.E. Wieman, Production of two overlapping Bose–Einstein condensates by sympathetic cooling, Phys. Rev. Lett. 78 (1997) 586–589.
[30] James Serrin, Henghui Zou, Existence of positive solutions of the Lane–Emden system, Atti Sem. Mat. Fis. Univ. Modena 46 (Suppl.) (1998) 369–380.
[31] Boyan Sirakov, Least energy solitary waves for a system of nonlinear Schrödinger equations in $\mathbf{R}^n$, Comm. Math. Phys. 271 (1) (2007) 199–221.
[32] J. Stenger, S. Inouye, D.M. Stamper-Kurn, H.-J. Miesner, A.P. Chikkatur, W. Ketterle, Spin domains in ground-state Bose–Einstein condensates, Nature 396 (6709) (1998) 345–348.
[33] E. Timmermans, Phase separation of Bose–Einstein condensates, Phys. Rev. Lett. 81 (1998) 5718–5721.
[34] Juncheng Wei, Tobias Weth, Nonradial symmetric bound states for a system of coupled Schrödinger equations, Atti Accad. Naz. Lincei Cl. Sci. Fis. Mat. Natur. Rend. Lincei (9) Mat. Appl. 18 (3) (2007) 279–293.
[35] Juncheng Wei, Tobias Weth, Asymptotic behaviour of solutions of planar elliptic systems with strong competition, Nonlinearity 21 (2) (2008) 305–317.
[36] Juncheng Wei, Tobias Weth, Radial solutions and phase separation in a system of two coupled Schrödinger equations, Arch. Ration. Mech. Anal. 190 (1) (2008) 83–106.